

IES

JOURNAL OF
ENVIRONMENTAL
SCIENCES

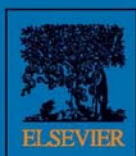
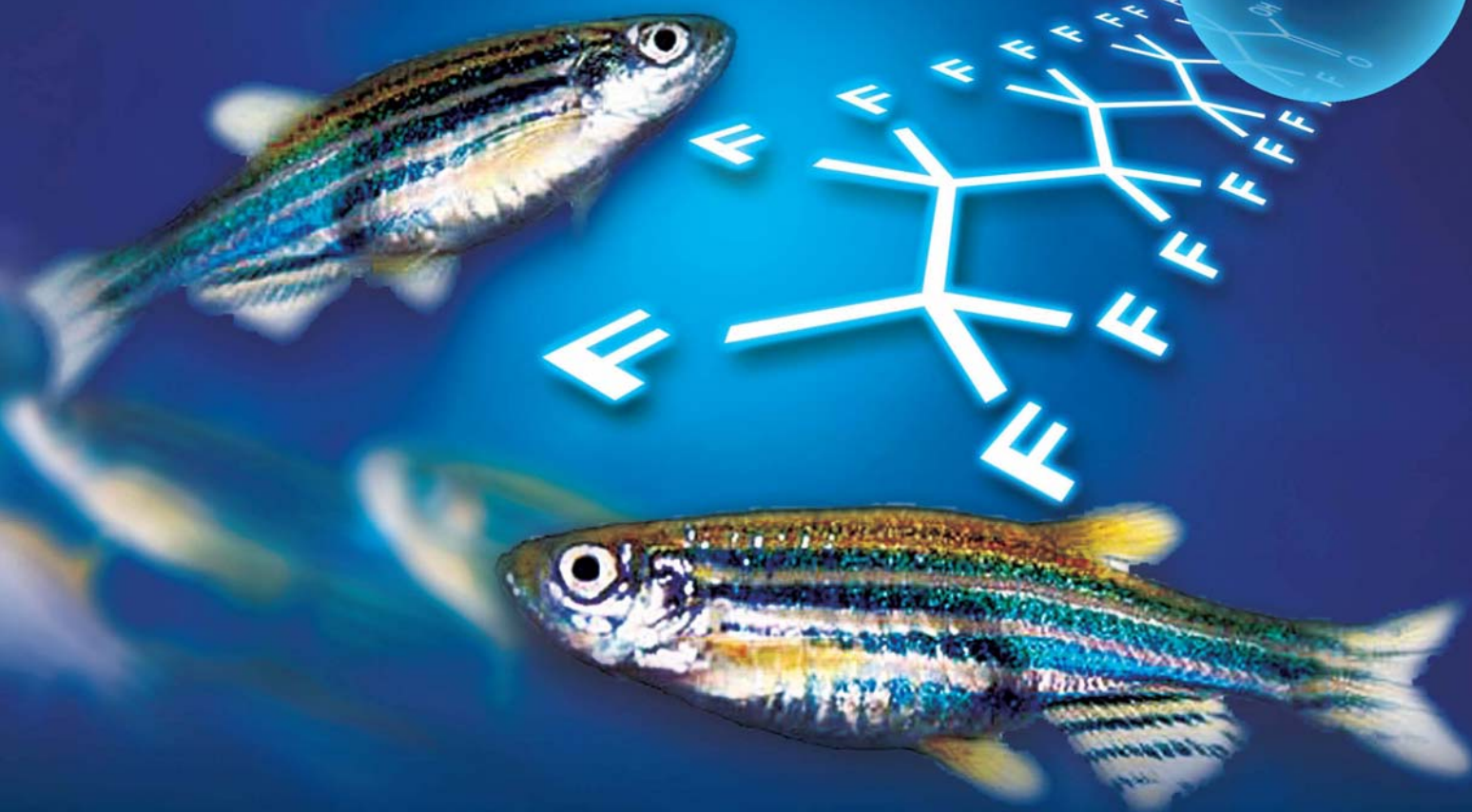
June 1, 2015 Volume 32
www.jesc.ac.cn

ISSN 1001-0742
CN 11-2629/X

PFNA

PFNA

PFNA



Sponsored by
Research Center for Eco-Environmental Sciences
Chinese Academy of Sciences

Highlight article

- 249 Cyanobacterial bloom dynamics in Lake Taihu
Katherine Z. Fu, Birget Moe, Xing-Fang Li and X. Chris Le

Regular articles

- 1 Membrane fouling controlled by coagulation/adsorption during direct sewage membrane filtration (DSMF) for organic matter concentration
Hui Gong, Zhengyu Jin, Xian Wang and Kaijun Wang
- 8 Photodegradation of methylmercury in Jialing River of Chongqing, China
Rongguo Sun, Dingyong Wang, Wen Mao, Shibo Zhao and Cheng Zhang
- 15 Powdered activated carbon adsorption of two fishy odorants in water: Trans,trans-2,4-heptadienal and trans,trans-2,4-decadienal
Xin Li, Jun Wang, Xiaojian Zhang and Chao Chen
- 26 Toxic effects of perfluorononanoic acid on the development of Zebrafish (*Danio rerio*) embryos
Hui Liu, Nan Sheng, Wei Zhang and Jiayin Dai
- 35 Denitrification and biofilm growth in a pilot-scale biofilter packed with suspended carriers for biological nitrogen removal from secondary effluent
Yunhong Shi, Guangxue Wu, Nan Wei and Hongying Hu
- 42 Groundwater arsenic removal by coagulation using ferric(III) sulfate and polyferric sulfate: A comparative and mechanistic study
Jinli Cui, Chuanyong Jing, Dongsheng Che, Jianfeng Zhang and Shuxuan Duan
- 54 Diurnal and spatial variations of soil NO_x fluxes in the northern steppe of China
Bing Wang, Xinqing Lee, Benny K.G. Theng, Jianzhong Cheng and Fang Yang
- 62 Effects of elevated atmospheric CO₂ concentration and temperature on the soil profile methane distribution and diffusion in rice-wheat rotation system
Bo Yang, Zhaozhi Chen, Man Zhang, Heng Zhang, Xuhui Zhang, Genxing Pan, Jianwen Zou and Zhengqin Xiong
- 72 The potential leaching and mobilization of trace elements from FGD-gypsum of a coal-fired power plant under water re-circulation conditions
Patricia Córdoba, Iria Castro, Mercedes Maroto-Valer and Xavier Querol
- 81 Unraveling the size distributions of surface properties for purple soil and yellow soil
Ying Tang, Hang Li, Xinmin Liu, Hualing Zhu and Rui Tian
- 90 Prediction of effluent concentration in a wastewater treatment plant using machine learning models
Hong Guo, Kwanho Jeong, Jiyeon Lim, Jeongwon Jo, Young Mo Kim, Jong-pyo Park, Joon Ha Kim and Kyung Hwa Cho
- 102 Cu-Mn-Ce ternary mixed-oxide catalysts for catalytic combustion of toluene
Hanfeng Lu, Xianxian Kong, Haifeng Huang, Ying Zhou and Yinfei Chen
- 108 Immobilization of self-assembled pre-dispersed nano-TiO₂ onto montmorillonite and its photo-catalytic activity
Tingting Zhang, Yuan Luo, Bing Jia, Yan Li, Lingling Yuan and Jiang Yu
- 118 Effects of fluoride on the removal of cadmium and phosphate by aluminum coagulation
Ruiping Liu, Bao Liu, Lijun Zhu, Zan He, Jiawei Ju, Huachun Lan and Huijuan Liu

CONTENTS

- 126 Structure and function of rhizosphere and non-rhizosphere soil microbial community respond differently to elevated ozone in field-planted wheat
Zhan Chen, Xiaoke Wang and He Shang
- 135 Chemical looping combustion: A new low-dioxin energy conversion technology
Xiuning Hua and Wei Wang
- 146 Picoplankton and virioplankton abundance and community structure in Pearl River Estuary and Daya Bay, South China
Zhixin Ni, Xiaoping Huang and Xia Zhang
- 155 Chemical characterization of size-resolved aerosols in four seasons and hazy days in the megacity Beijing of China
Kang Sun, Xingang Liu, Jianwei Gu, Yunpeng Li, Yu Qu, Junling An, Jingli Wang, Yuanhang Zhang, Min Hu and Fang Zhang
- 168 Numerical study of the effects of Planetary Boundary Layer structure on the pollutant dispersion within built-up areas
Yucong Miao, Shuhua Liu, Yijia Zheng, Shu Wang, Zhenxin Liu and Bihui Zhang
- 180 Interaction between Cu^{2+} and different types of surface-modified nanoscale zero-valent iron during their transport in porous media
Haoran Dong, Guangming Zeng, Chang Zhang, Jie Liang, Kito Ahmad, Piao Xu, Xiaoxiao He and Mingyong Lai
- 189 Tricrystalline TiO_2 with enhanced photocatalytic activity and durability for removing volatile organic compounds from indoor air
Kunyang Chen, Lihong Zhu and Kun Yang
- 196 Biogenic volatile organic compound analyses by PTR-TOF-MS: Calibration, humidity effect and reduced electric field dependency
Xiaobing Pang
- 207 Enhancement of elemental mercury adsorption by silver supported material
Rattabal Khunphonoi, Pummarin Khamdagsag, Siriluk Chiarakorn, Nurak Grisdanurak, Adjana Paerungruang and Somrudee Predapitakkun
- 217 Characterization of soil fauna under the influence of mercury atmospheric deposition in Atlantic Forest, Rio de Janeiro, Brazil
Andressa Cristhy Buch, Maria Elizabeth Fernandes Correia, Daniel Cabral Teixeira and Emmanoel Vieira Silva-Filho
- 228 Particle size distribution and characteristics of heavy metals in road-deposited sediments from Beijing Olympic Park
Haiyan Li, Anbang Shi and Xiaoran Zhang
- 238 Mesoporous carbon adsorbents from melamine-formaldehyde resin using nanocasting technique for CO_2 adsorption
Chitrakshi Goel, Haripada Bhunia and Pramod K. Bajpai

Available online at www.sciencedirect.com

ScienceDirect

www.journals.elsevier.com/journal-of-environmental-sciences

Tricrystalline TiO₂ with enhanced photocatalytic activity and durability for removing volatile organic compounds from indoor air

Kunyang Chen^{1,2}, Lizhong Zhu^{1,2,*}, Kun Yang^{1,2}

1. Department of Environmental Science, Zhejiang University, Hangzhou 310058, China. E-mail: zljz@zju.edu.cn

2. Zhejiang Provincial Key Laboratory of Organic Pollution Process and Control, Hangzhou 310058, China

ARTICLE INFO

Article history:

Received 20 September 2014

Revised 24 October 2014

Accepted 30 October 2014

Available online 21 April 2015

Keywords:

VOC

Photocatalysis

Tricrystalline TiO₂

Nanomaterials

Mesoporous

Gaseous

ABSTRACT

It is important to develop efficient and economic techniques for removing volatile organic compounds (VOCs) in indoor air. Heterogeneous TiO₂-based semiconductors are a promising technology for achieving this goal. Anatase/brookite/rutile tricrystalline TiO₂ with mesoporous structure was synthesized by a low-temperature hydrothermal route in the presence of HNO₃. The obtained samples were characterized by X-ray diffraction and N₂ adsorption–desorption isotherm. The photocatalytic activity was evaluated by photocatalytic decomposition of toluene in air under UV light illumination. The results show that tricrystalline TiO₂ exhibited higher photocatalytic activity and durability toward gaseous toluene than bicrystalline TiO₂, due to the synergistic effects of high surface area, uniform mesoporous structure and junctions among mixed phases. The tricrystalline TiO₂ prepared at R_{HNO₃} = 0.8, containing 80.7% anatase, 15.6% brookite and 3.7% rutile, exhibited the highest photocatalytic activity, about 3.85-fold higher than that of P25. The high activity did not significantly degrade even after five reuse cycles. In conclusion, it is expected that our study regarding gas-phase degradation of toluene over tricrystalline TiO₂ will enrich the chemistry of the TiO₂-based materials as photocatalysts for environmental remediation and stimulate further research interest on this intriguing topic.

© 2015 The Research Center for Eco-Environmental Sciences, Chinese Academy of Sciences.

Published by Elsevier B.V.

Introduction

Volatile organic compounds (VOCs) are a group comprising the most abundant organic pollutants in indoor air, with concentrations ranging from 0.005 to 4600 µg/m³ (Barro et al., 2009). They are emitted from various sources such as combustion by-products, cooking, construction materials, office equipment, and consumer products (Gallego et al., 2008; Weschler, 2009). Many VOCs are toxic or carcinogenic to humans, even at low concentrations (Missia et al., 2010). For instance, exposure to formaldehyde, benzene or toluene may cause skin irritation,

rhinitis, headache, fatigue, and allergic reactions (Bernstein et al., 2008; Gallego et al., 2009); and benzene derived from aromatic molecules can show carcinogenic or mutagenic activity (Missia et al., 2010).

A number of techniques have been developed to remove VOCs from indoor air, such as adsorption techniques and oxidation techniques (Parmar and Rao, 2009). The former are conventional methods; gaseous pollutants are transferred from air to a solid phase with various adsorbents, e.g., activated carbon (Liu et al., 2004). In contrast, heterogeneous photocatalysis using semiconductors as photocatalysts, an advanced oxidation

* Corresponding author.

technique, has greater potential. In the photocatalytic processes, an array of VOCs can be destroyed and even completely mineralized into CO_2 and H_2O (Demeestere et al., 2007; Nakata and Fujishima, 2012). While compared to other oxidation technologies like electron beam and plasma treatments, heterogeneous photocatalysis is more effective and economical, and suitable for wider application scope.

Among all semiconductor photocatalysts, TiO_2 (primarily existing in three crystal phases, i.e., anatase, brookite, and rutile) is the most efficient and applicable, because of its wide band-gap energy, durability against photocorrosion, low toxicity and low cost (Demeestere et al., 2007; Wang et al., 2007). However, the photocatalytic applications of TiO_2 are limited by its low quantum efficiency due to the fast recombination between the photogenerated electrons and holes (Chen and Mao, 2007). The formation of phase junctions has been demonstrated as an effective strategy for inhibiting photogenerated electron-hole recombination (Li and Gray, 2007). In practice, tricrystalline TiO_2 has been synthesized by thermohydrolysis of TiCl_4 (Di Paola et al., 2008, 2009) and with solvothermal treatment of titanium tetrabutoxide (TBOT) in toluene (Liao et al., 2012). In the aqueous phase, the tricrystalline TiO_2 exhibited higher photocatalytic activity for organic pollutants than bicrystalline TiO_2 .

However, the photocatalytic performance and durability of tricrystalline TiO_2 have not been tested in the gas phase. Due to the accumulation of strongly bound reaction intermediates on the TiO_2 surface (Demeestere et al., 2007; Hu et al., 2006), deactivation of TiO_2 during photodegradation of organic pollutants was much more frequently observed in the gas phase than the aqueous phase. Additionally, the existing methods for synthesizing tricrystalline TiO_2 are energy-consuming, and usually require high-temperature ($\geq 400^\circ\text{C}$) (Lopez et al., 2001), long-time (≥ 48 hr) treatments (Di Paola et al., 2008, 2009), or toxic toluene (Liao et al., 2012).

In this study, we aim to promote the application of tricrystalline TiO_2 in photocatalytic elimination of indoor VOCs. Anatase/brookite/rutile tricrystalline TiO_2 was synthesized using a low-temperature hydrothermal method with the assistance of HNO_3 . The photocatalytic activity and durability in the photodegradation of toluene were analyzed and compared to P25 TiO_2 (a widely used benchmark model photocatalyst). Toluene is one of the most abundant VOCs found in indoor air (Greenberg, 1997; Wang et al., 2007) and is not easily degraded due to the relative stability of its aromatic ring against oxidation and reduction processes (Hodgson et al., 2007).

1. Materials and methods

1.1. Synthesis

Anatase/brookite/rutile tricrystalline TiO_2 was prepared as follows. 4.4 mL TBOT (Aladdin Reagent Co.) was slowly added to 50 mL of a 10 mol/L NaOH solution under vigorous stirring, yielding an amorphous TiO_2 suspension. After 5 hr stirring, the suspension was separated by centrifugation, washed three times with deionized water and redispersed in 39 mL deionized water. Then, a concentrated HNO_3 solution (65%) was added under stirring. The molar ratios of HNO_3 to TBOT (R_{HNO_3}) were

varied from 0.2 to 1.2 at intervals of 0.2 by varying the volume of HNO_3 solution. The mixture was sealed in a Teflon autoclave and maintained at 180°C for 24 hr. Finally, the resulting precipitate was separated by centrifugation, washed with deionized water until the washing solution reached pH 7 and then dried at 50°C . The TiO_2 powders were labeled as TiO_2 -a. For example, TiO_2 nanocrystals prepared at $R_{\text{HNO}_3} = 0.8$ were denoted as TiO_2 -0.8.

1.2. Characterization

The synthesized products were characterized in three aspects, including the X-ray diffraction (XRD) pattern, specific surface area and pore size distribution. First, the XRD patterns were explored between 20° and 90° (2θ range, $\Delta 2\theta = 0.02^\circ$) with a D/MAX 2550 PC using $\text{Cu K}\alpha$ radiation (Rigaku, Tokyo, Japan). The phase contents of the TiO_2 samples were calculated from the integrated intensities of anatase (101), rutile (110), and brookite (121) peaks (Luo et al., 2003; Zhang and Banfield, 2000). The average diameters (d) of the crystallites (i.e., anatase, rutile and brookite) were calculated from the full-width at half-maximum of the respective XRD patterns using the Scherrer formula (Patterson, 1939). Second, the specific surface areas were estimated using N_2 adsorption experiments based on the classical Brunauer–Emmett–Teller (BET) method, which were conducted in the relative pressure range of 0.01 to 0.1 with a NOVA 2000e surface area analyzer (Quantachrome, Florida, U.S.A.). The pore size distributions of the TiO_2 nanocrystals were calculated from the desorption branch of the nitrogen isotherms using the Barrett–Joyner–Halenda (BJH) method (Barrett et al., 1951).

1.3. Photocatalytic activity

The photocatalytic activity of tricrystalline TiO_2 was evaluated by the photocatalytic degradation of toluene in air under UV irradiation, with P25 as a reference. The photodegradation of gaseous toluene was conducted in a cylindrical quartz photoreactor operating in continuous flow mode (Fig. 1). The carrier gas generated from a clean-air generator was split into three streams. The first stream was bubbled through water to set the humidity for the reaction ($20\% \pm 3\%$), and the second stream was used to generate a gaseous stream of toluene passed through a permeation tube filled with pure liquid toluene cooled in an ice-water bath. These two streams then converged with the clean air branch (the third stream) in a 1.5 L-cylindrical-chamber. The toluene/air mixed vapor was fed to the catalyst dish at a total flow rate of 1 L/min, and the concentration of toluene was 1 ppm, which is a typical level in indoor air environments. The catalyst dish was prepared by coating 20 mg of TiO_2 onto a piece of quartz wool with an area of $11 \times 20 \text{ cm}^2$ using 20 mL of a TiO_2 /ethanol suspension. A 6 W UV lamp with a dominant wavelength of 254 nm was used as the irradiation source. The distance between the catalyst dish and the lamp was 1.5 cm. The concentrations of toluene were determined using an online gas chromatograph (GC, Fuli 9790, Wenling, China) equipped with a stainless steel packed column (2.5% dinonyl phthalate + 2.5% bentane, length: 3 m, diameter: 3 mm) and a flame ionization detector. Prior to photodegradation, adsorption equilibrium of toluene on the photocatalyst was achieved in 4 hr without irradiation.

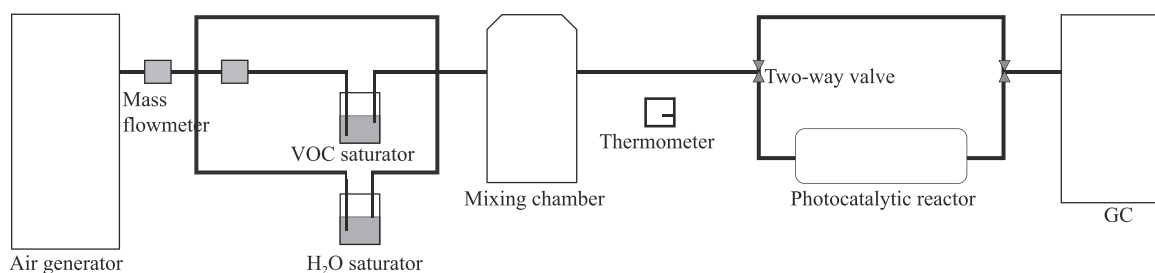


Fig. 1 – Photocatalytic device. (1) Air generator; (2) mass flowmeter; (3) VOC saturator; (4) H₂O saturator; (5) mixing chamber; (6) thermometer; (7) Two-way valve; (8) photocatalytic reactor; (9) GC.

The photodegradation rate of toluene was calculated by the following equation:

$$\eta_t = \frac{C_0 - C}{C_0} \times 100\% \quad (1)$$

where η_t (%) represents the photodegradation rate at reaction time t , C_0 (mg/m³) and C (mg/m³) are the initial and the reaction concentration of toluene, respectively. The photocatalytic degradation of toluene on TiO₂ is a pseudo-first-order reaction and its kinetics can be expressed as follows (Demeestere et al., 2007):

$$\ln\left(\frac{C_0}{C}\right) = k_{app}t$$

where, k_{app} (min⁻¹) represents the apparent kinetic constant.

1.4. Hydroxyl radicals

In order to explore the synergistic effects of anatase–brookite–rutile phases, the formation of hydroxyl radicals (OH) during the UV irradiation of TiO₂ nanocrystals was studied. The amount of OH radicals generated on the surface of UV-irradiated TiO₂ was measured with the terephthalic acid (TA, Aladdin Reagent Co., Shanghai, China) fluorescence probe method (Hirakawa and Nosaka, 2002; Ishibashi et al., 2000b). TiO₂ 5 mg was suspended in 50 mL of an aqueous solution containing 2 mmol/L NaOH and 0.5 mmol/L TA. The suspension was stirred in darkness for 30 min. Then, 3 mL of the suspension was exposed to UV light irradiation at a wavelength of 254 nm (using a 6-W UV lamp as the light source) for 5 min, followed by filtration through a 0.25 μm membrane filter. Finally, the fluorescence signal of 2-hydroxy terephthalic acid (TAOH) at 426 nm was recorded on a RF-5301pc spectrofluorophotometer (Shimadzu, Tokyo, Japan) at an excitation wavelength of 320 nm.

1.5. Photocatalytic durability

To explore the photocatalytic long-term durability advantage of the TiO₂ samples with the highest photocatalytic activity, five reuse cycles were tested for the photodegradation of gaseous toluene. Each cycle included 2 hr of light on and 4 hr of light off.

The possible gaseous intermediates (Demeestere et al., 2007), such as benzene, phenol benzaldehyde, benzyl alcohol and benzoic acid, were analyzed by collecting air samples at the reactor outlet in stainless steel tubes packed with 300 mg activated carbon during the photodegradation. The absorbed

intermediates were extracted into carbon disulfide and measured by GC. CO₂ was converted into methane in a converter with nickel catalysts at a temperature of 350°C and also determined on the online GC. The concentration of toluene was maintained at 100 ppm in the intermediate and CO₂ identification tests, in order to improve the accuracy of test results.

2. Results and discussion

2.1. Phase composition

The phase compositions of the obtained samples were sensitive to the molar ratios of HNO₃ to TBOT (R_{HNO_3}). The XRD patterns show that the samples obtained at R_{HNO_3} between 0.8 and 1.2 were anatase/brookite/rutile three-phase TiO₂ nanocrystals (Fig. 2). According to the standard diffraction data, the characteristic 2θ values at around 25.3°, 30.8° and 27.4° corresponded to the anatase (101) plane (JCPDS No. 21-1272), the brookite (121) plane (JCPDS No. 29-1360) and the rutile (110) plane (JCPDS No. 21-1276), respectively. The anatase content increased from 26.0% to 80.7% and the rutile content decreased from 54.8% to 3.7% when R_{HNO_3} decreased from 1.2 to 0.8, whereas the brookite

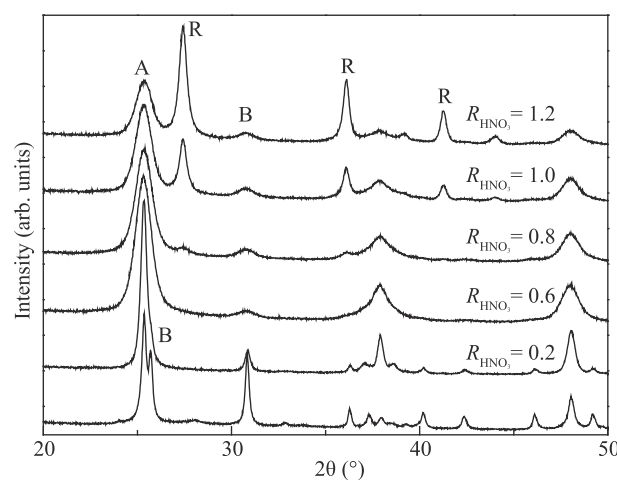


Fig. 2 – XRD patterns of TiO₂ nanocrystals. Peaks of anatase, brookite and rutile are identified as A, B and R, respectively. R_{HNO_3} is molar ratio of HNO₃ to titanium tetrabutoxide (TBOT) during the production process of TiO₂ nanocrystals.

Table 1 – Physicochemical properties of TiO₂ nanocrystals and P25.

R_{HNO_3} ^a	Anatase ^b (%)	Brookite ^b (%)	Rutile ^b (%)	d (anatase) ^b (nm)	d (brookite) ^b (nm)	d (rutile) ^b (nm)	S_{BET} (m ² /g [−])	Pore size ^c (nm)
1.2	26.0	19.2	54.8	19.2	8.70	23.3	92.10	8.6
1.0	59.5	14.5	26.0	8.60	7.60	21.3	112.9	6.3
0.8	80.7	15.6	3.70	8.20	7.50	19.2	136.6	5.4
P25	80.0	–	20.0	25.0	–	35.0	58.00	7.1

^a Molar ratio of HNO₃ to titanium tetrabutoxide (TBOT) during the production process of TiO₂ nanocrystals.

^b Determined by X-ray diffraction (XRD) patterns.

^c Estimated using the desorption branch of the N₂ adsorption/desorption isotherm and the Barrett-Joyner-Halenda (BJH) formula.

content remained relatively steady (14.5–19.2%) (Table 1). These trends are consistent with previous reports (Tian et al., 2006; Yuan et al., 2004), which indicates that a dilute acid solution favored the formation of anatase, while a concentrated acid solution promoted the formation of rutile. The generation of the brookite phase might be attributed to the presence of Na⁺ ions (Shen et al., 2013). The above results demonstrate an effective approach to the controllable fabrication of tricrystalline TiO₂ with a low-temperature hydrothermal treatment.

2.2. Photocatalytic activity

As shown in Fig. 3a, at the beginning of irradiation, adsorbed toluene on TiO₂ was preferentially degraded, after which more toluene could be adsorbed and degraded. During this period, toluene reacted rapidly. As the concentration of toluene was constant, the adsorption equilibrium and degradation equilibrium were easily reached, and the photodegradation rate of toluene leveled off. The photodegradation rate of toluene did not decrease and no deactivation was observed during a 2-hr test. It is unlikely that the leveling-off phenomenon was due to deactivation of the catalysts by the remaining intermediates, because if intermediates remained and occupied the active sites of the TiO₂ surface, the photodegradation rate of toluene would have decreased rather than leveling off. It could be clearly observed that the final degradation sequence followed the same order of the rate constants (Fig. 3b), which initially increased with decreasing R_{HNO_3} and then decreased. Tricrystalline TiO₂-0.8

was proved to be the most efficient photocatalyst, with a photodegradation conversion of 89% and an apparent kinetic constant of $9.3 \times 10^{-2} \text{ min}^{-1}$. In contrast, P25 only showed a photodegradation conversion of 44% and an apparent kinetic constant of $24 \times 10^{-3} \text{ min}^{-1}$. Moreover, a decrease in the activity of tricrystalline TiO₂ was observed when R_{HNO_3} became larger than 0.8, during which the ratio of anatase-brookite-rutile shifted away from its optimum.

Two factors are essential during gas-solid photocatalysis: the adsorption of pollutant molecules and the separation/transport of electrons and holes. The adsorption is usually related to the surface area and the pore structure of TiO₂. The tricrystalline TiO₂-0.8 had the largest surface area (136.6 m²/g) because it had the smallest crystallite size (Table 1). Also, this TiO₂ nanomaterial exhibited a type IV isotherm with a hysteresis loop of type H2 over the relative pressure range of 0.5 to 0.8 (Fig. 4), indicating the presence of ink-bottle-like pores with narrow necks and wider bodies (Dai et al., 2012; Yu et al., 2003). These mesopores resulted from the aggregation of primary particles, with the smallest average pore size of approximately 5.4 nm (Fig. 4). A larger surface area favors TiO₂ adsorbing more gaseous reactants, such as H₂O, O₂ and organic pollutants, onto the surface, and the uniform mesopores allow for the rapid diffusion of these reactants and various products during the photocatalytic reaction, thereby enhancing the photocatalytic activity (Ismail and Bahnemann, 2011; Yu et al., 2006). However, the kinetic constant with normalized by surface area for tricrystalline TiO₂ ($0.68 \times 10^{-3} \text{ g}/(\text{min} \cdot \text{m}^2)$) was still

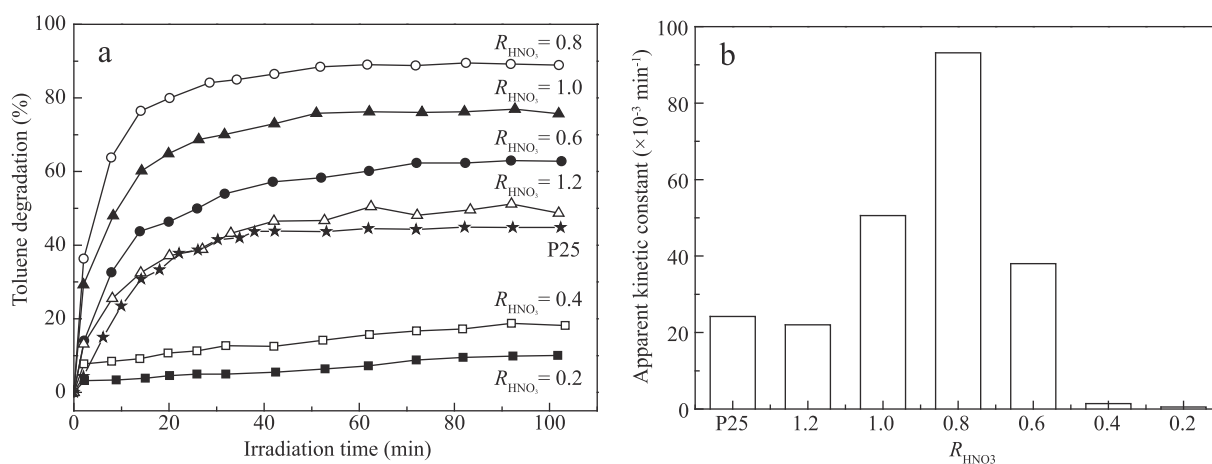


Fig. 3 – Photodegradation of gaseous toluene on TiO₂ nanocrystals and P25 as degradation rate (a) and apparent kinetic constant (b).

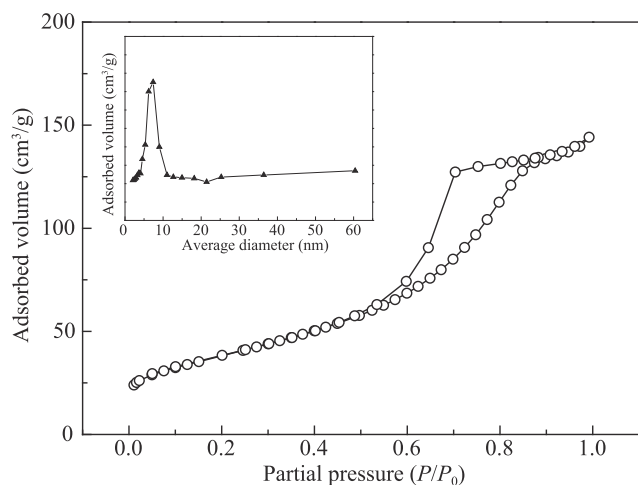


Fig. 4 – Nitrogen adsorption–desorption isotherm of tricrystalline $\text{TiO}_2\text{-0.8}$. The inset was the pore size distribution curve calculated from the desorption branch of the nitrogen isotherm using the BJH method.

higher than that of P25 ($0.42 \times 10^{-3} \text{ g}/(\text{min}\cdot\text{m}^2)$), clearly demonstrating that surface area is not the only influential factor for photocatalytic activity in this system.

Therefore, the other crucial factor for enhancing the photocatalytic activity of TiO_2 is the efficient charge separation and transfer, which could be evaluated by the formation of $\cdot\text{OH}$ radicals during the UV irradiation of TiO_2 nanocrystals in TA solutions (Lv et al., 2010; Xiang et al., 2010; Yu et al., 2009). The absorption of a photon with energy higher than the band gap energy results in the formation of a valence band hole and a conduction band electron. It is commonly acknowledged that adsorbed water or hydroxide ions can be trapped by the holes to produce $\cdot\text{OH}$ radicals, which are known to be a strong oxidizing species. Electrons are trapped at the surface after reacting with adsorbed molecular oxygen to produce superoxide anion radicals, which then form more $\cdot\text{OH}$ radicals. The yield of $\cdot\text{OH}$ radicals depends on the competition between the above reactions and electron-hole recombination. Therefore, the higher the formation rate of $\cdot\text{OH}$ radicals, the higher the separation efficiency of electron-hole pairs achieved can be. Fig. 5 shows the changes in fluorescence spectra with irradiation time for TA solutions. No increase in fluorescence intensity was observed in the absence of UV light or TiO_2 nanocrystals, indicating that the fluorescence was caused by the chemical reaction of TA with $\cdot\text{OH}$ that formed on the TiO_2 /water interface via photocatalytic reactions (Hirakawa et al., 2007; Ishibashi et al., 2000a). On the contrary, in the presence of TiO_2 nanocrystals, the fluorescence intensity as a result of UV irradiation in TA solutions increased linearly as a function of time. Thus, it could be inferred that the number of $\cdot\text{OH}$ radicals produced at the TiO_2 surface was proportional to the irradiation time and that this reaction obeyed zero-order reaction rate kinetics. Tricrystalline $\text{TiO}_2\text{-0.8}$ showed a much greater formation rate than P25, suggesting that the three-phase composite (anatase/brookite/rutile) enhanced the production of $\cdot\text{OH}$ radicals. The two-phase structure of anatase and rutile with a suitable ratio has been reported to be beneficial in reducing the recombination rate of photo-generated electrons and holes, thereby enhancing the

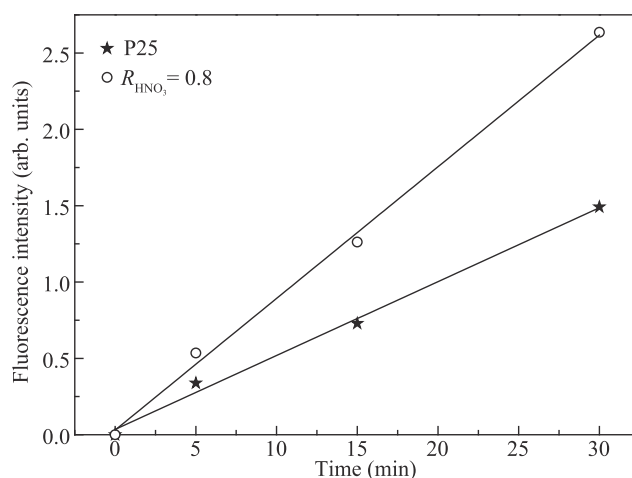


Fig. 5 – Fluorescence intensity changes observed during the irradiation of tricrystalline $\text{TiO}_2\text{-0.8}$ and P25 in a 0.5 mmol/L aqueous NaOH solution of terephthalic acid (excitation at 320 nm).

rate of $\cdot\text{OH}$ formation (Lv et al., 2010). This enhancing relationship also applies to tricrystalline TiO_2 . The coupled anatase, brookite and rutile phases possessed different redox energies for their corresponding conduction and valence bands (Shibata et al., 2004; Yin et al., 2010). Heterojunctions were thus formed, allowing an easier transfer of photogenerated electrons from one phase to another, which could suppress the recombination of photogenerated electrons and holes and consequently enhance the production of $\cdot\text{OH}$ radicals. In summary, the high photocatalytic activity of tricrystalline $\text{TiO}_2\text{-0.8}$ could be attributed to the combined effects of high specific surface area, uniform mesoporous structure and junctions among mixed phases.

2.3. Photocatalytic durability

The toluene conversion on tricrystalline $\text{TiO}_2\text{-0.8}$ was maintained at $89\% \pm 1\%$ without significant deactivation for up to five repeated cycles, while P25 gradually lost its activity (Fig. 6). A

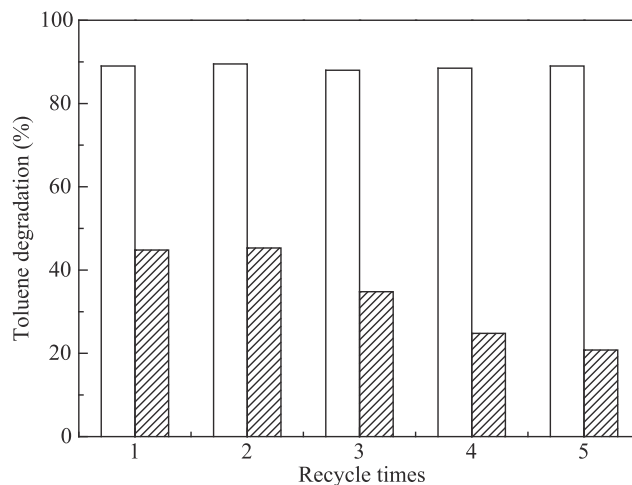


Fig. 6 – Recycling test over tricrystalline $\text{TiO}_2\text{-0.8}$ (blank) and P25 (filled) for five repeat uses.

Table 2 – Comparison of intermediates and CO₂ resulted from toluene degradation by tricrystalline TiO₂-0.8 and P25.

R _{HNO₃}	Intermediates ^a (mg/m ³)			CO ₂ yield (%)
	Benzyl alcohol	Benzaldehyde	Benzoic acid	
0.8	0.17	42.00	n.d. ^b	56.3
P25	0.61	376.4	0.01	20.9

^a Concentrations of intermediates in the extracts.
^b Not detected.

color change of P25 from white to yellow was observed after the third reuse cycle. These results could be attributed to the more effective decomposition of toluene and refractory intermediates by the tricrystalline TiO₂-0.8. As intermediates, benzyl alcohol and benzaldehyde were identified for both tricrystalline TiO₂-0.8 and P25, whereas benzoic acid was identified only for P25 (Table 2). It is clear that the oxidation of toluene took place at the methyl group for both photocatalysts. The concentrations of three main intermediates for tricrystalline TiO₂-0.8 were much lower than those for P25, while the yield of CO₂ for tricrystalline TiO₂ was higher than that for P25 (56.3% and 20.9%, respectively), confirming that tricrystalline TiO₂-0.8 enhanced the photocatalytic degradation of both toluene and its intermediates.

In an attempt to increase the TiO₂ lifetime, other researchers have carried out catalyst regeneration, focusing on the destruction of presumed intermediates. Two main types of regeneration methods have been reported (Cao et al., 2000; Demeestere et al., 2007; Lewandowski and Ollis, 2003). First, thermal regeneration of TiO₂ deactivated after toluene degradation was applied (Cao et al., 2000). Temperatures as high as 420°C for at least 2 hr were required to “burn out” strongly bound intermediates and to recover the initial activity completely. A second type of regeneration method involves exposure of deactivated TiO₂ to contaminant-free, humidified air and UV irradiation (Lewandowski and Ollis, 2003). However, these methods require high regeneration temperature or long regeneration time, costing much energy. Based on the photocatalytic activity and reuse tests, this tricrystalline TiO₂-0.8 was not only highly efficient but also quite durable for prolonged use.

3. Conclusions

With the assistance of HNO₃, anatase/brookite/rutile tricrystalline TiO₂ with high crystallinity, large surface area (136.6 m²/g) and uniform mesopores (5.4 nm) was successfully prepared using a low-temperature hydrothermal method. Compared to the existing methods, this route was more energy-saving, and the phase structure could be finely controlled by adjusting the amount of HNO₃. The three-phase TiO₂ nanocrystals showed much higher photocatalytic activity and durability in the degradation of gaseous toluene than the commercial anatase/rutile P25, mainly because of their superior properties in the adsorption of pollutant molecules and the separation/transport of electrons and holes. It is expected that our study regarding gas-phase degradation of toluene over tricrystalline TiO₂ can enrich the chemistry of TiO₂-based

materials as photocatalysts for environmental remediation and stimulate further research interest on this intriguing topic.

Acknowledgments

This work was supported by grants from the National High Technology Research and Development Program (863) of China (Nos. 2010AA064902 and 2012AA062702) and the Key Innovation Team for Science and Technology of Zhejiang Province (No. 2009R50047).

REFERENCES

- Barrett, E.P., Joyner, L.G., Halenda, P.P., 1951. The determination of pore volume and area distributions in porous substances. 1. Computations from nitrogen isotherms. *J. Am. Chem. Soc.* 73 (1), 373–380.
- Barro, R., Regueiro, J., Llompard, M., Garcia-Jares, C., 2009. Analysis of industrial contaminants in indoor air: part 1. Volatile organic compounds, carbonyl compounds, polycyclic aromatic hydrocarbons and polychlorinated biphenyls. *J. Chromatogr. A* 1216 (3), 540–566.
- Bernstein, J.A., Alexis, N., Bacchus, H., Bernstein, I.L., Fritz, P., Horner, E., et al., 2008. The health effects of nonindustrial indoor air pollution. *J. Allergy Clin. Immunol.* 121 (3), 585–591.
- Cao, L., Gao, Z., Suib, S.L., Obee, T.N., Hay, S.O., Freihaut, J.D., 2000. Photocatalytic oxidation of toluene on nanoscale TiO₂ catalysts: studies of deactivation and regeneration. *J. Catal.* 196 (2), 253–261.
- Chen, X., Mao, S.S., 2007. Titanium dioxide nanomaterials: synthesis, properties, modifications, and applications. *Chem. Rev.* 107 (7), 2891–2959.
- Dai, G.T., Zhao, L., Wang, S.M., Hu, J.H., Dong, B.H., Lu, H.B., Li, J., 2012. Double-layer composite film based on sponge-like TiO₂ and P25 as photoelectrode for enhanced efficiency in dye-sensitized solar cells. *J. Alloys Compd.* 539, 264–270.
- Demeestere, K., Dewulf, J., Van Langenhove, H., 2007. Heterogeneous photocatalysis as an advanced oxidation process for the abatement of chlorinated, monocyclic aromatic and sulfurous volatile organic compounds in air: state of the art. *Crit. Rev. Environ. Sci. Technol.* 37 (6), 489–538.
- Di Paola, A., Cufalo, G., Addamo, M., Ellardita, M.B., Campostrini, R., Ischia, M., et al., 2008. Photocatalytic activity of nanocrystalline TiO₂ (brookite, rutile and brookite-based) powders prepared by thermohydrolysis of TiCl₄ in aqueous chloride solutions. *Colloids Surf. A* 317 (1–3), 366–376.
- Di Paola, A., Bellardita, M., Ceccato, R., Palmisano, L., Parrino, F., 2009. Highly active photocatalytic TiO₂ powders obtained by thermohydrolysis of TiCl₄ in water. *J. Phys. Chem. C* 113 (34), 15166–15174.
- Gallego, E., Roca, F.X., Guardino, X., Rosell, M.G., 2008. Indoor and outdoor BTX levels in Barcelona City metropolitan area and Catalan rural areas. *J. Environ. Sci.* 20 (9), 1063–1069.
- Gallego, E., Roca, X., Perales, J.F., Guardino, X., 2009. Determining indoor air quality and identifying the origin of odour episodes in indoor environments. *J. Environ. Sci.* 21 (3), 333–339.
- Greenberg, M.M., 1997. The central nervous system and exposure to toluene: a risk characterization. *Environ. Res.* 72 (1), 1–7.
- Hirakawa, T., Nosaka, Y., 2002. Properties of O₂^{•−} and OH[•] formed in TiO₂ aqueous suspensions by photocatalytic reaction and the influence of H₂O₂ and some ions. *Langmuir* 18 (8), 3247–3254.
- Hirakawa, T., Yawata, K., Nosaka, Y., 2007. Photocatalytic reactivity for O₂^{•−} and OH[•] radical formation in anatase and rutile TiO₂ suspension as the effect of H₂O₂ addition. *Appl. Catal. A Gen.* 325 (1), 105–111.

- Hodgson, A.T., Destailats, H., Sullivan, D.P., Fisk, W.J., 2007. Performance of ultraviolet photocatalytic oxidation for indoor air cleaning applications. *Indoor Air* 17 (4), 305–316.
- Hu, C., Lin, L.Y., Hu, X.X., 2006. Morphology of metal nanoparticles photodeposited on TiO₂/silical gel and photothermal activity for destruction of ethylene. *J. Environ. Sci.* 18 (1), 76–82.
- Ishibashi, K., Fujishima, A., Watanabe, T., Hashimoto, K., 2000a. Detection of active oxidative species in TiO₂ photocatalysis using the fluorescence technique. *Electrochem. Commun.* 2 (3), 207–210.
- Ishibashi, K., Fujishima, A., Watanabe, T., Hashimoto, K., 2000b. Quantum yields of active oxidative species formed on TiO₂ photocatalyst. *J. Photochem. Photobiol. A Chem.* 134 (1–2), 139–142.
- Ismail, A.A., Bahnemann, D.W., 2011. Mesoporous titania photocatalysts: preparation, characterization and reaction mechanisms. *J. Mater. Chem.* 21 (32), 11686–11707.
- Lewandowski, M., Ollis, D.F., 2003. Extension of a two-site transient kinetic model of TiO₂ deactivation during photocatalytic oxidation of aromatics: concentration variations and catalyst regeneration studies. *Appl. Catal. B Environ.* 45 (3), 223–238.
- Li, G., Gray, K.A., 2007. The solid–solid interface: explaining the high and unique photocatalytic reactivity of TiO₂-based nanocomposite materials. *Chem. Phys.* 339 (1–3), 173–187.
- Liao, Y.L., Que, W.X., Jia, Q.Y., He, Y.C., Zhang, J., Zhong, P., 2012. Controllable synthesis of brookite/anatase/rutile TiO₂ nanocomposites and single-crystalline rutile nanorods array. *J. Mater. Chem.* 22 (16), 7937–7944.
- Liu, J., Huang, Z.H., Wang, Z.S., Kang, F.Y., 2004. Gas phase trichloroethylene removal at low concentration using activated carbon fiber. *J. Environ. Sci.* 26 (1), 53–55.
- Lopez, T., Gomez, R., Sanchez, E., Tzompantzi, F., Vera, L., 2001. Photocatalytic activity in the 2,4-dinitroaniline decomposition over TiO₂ sol–gel derived catalysts. *J. Sol-Gel Sci. Technol.* 22 (1–2), 99–107.
- Luo, H.M., Wang, C., Yan, Y.S., 2003. Synthesis of mesostructured titania with controlled crystalline framework. *Chem. Mater.* 15 (20), 3841–3846.
- Lv, K.L., Yu, J.G., Deng, K.J., Li, X.H., Li, M., 2010. Effect of phase structures on the formation rate of hydroxyl radicals on the surface of TiO₂. *J. Phys. Chem. Solids* 71 (4), 519–522.
- Missia, D.A., Demetriou, E., Michael, N., Tolis, E.I., Bartzis, J.G., 2010. Indoor exposure from building materials: a field study. *Atmos. Environ.* 44 (35), 4388–4395.
- Nakata, K., Fujishima, A., 2012. TiO₂ photocatalysis: design and applications. *J. Photochem. Photobiol. C* 13 (3), 169–189.
- Parmar, G.R., Rao, N., 2009. Emerging control technologies for volatile organic compounds. *Crit. Rev. Environ. Sci. Technol.* 39 (1), 41–78.
- Patterson, A.L., 1939. The Scherrer formula for X-ray particle size determination. *Phys. Rev.* 56, 978–982.
- Shen, X.J., Tian, B.Z., Zhang, J.L., 2013. Tailored preparation of titania with controllable phases of anatase and brookite by an alkaline hydrothermal route. *Catal. Today* 201, 151–158.
- Shibata, T., Irie, H., Ohmori, M., Nakajima, A., Watanabe, T., Hashimoto, K., 2004. Comparison of photochemical properties of brookite and anatase TiO₂ films. *Phys. Chem. Chem. Phys.* 6 (6), 1359–1362.
- Tian, B., Chen, F., Zhang, J., Anpo, M., 2006. Influences of acids and salts on the crystalline phase and morphology of TiO₂ prepared under ultrasound irradiation. *J. Colloid Interface Sci.* 303 (1), 142–148.
- Wang, S., Ang, H.M., Tade, M.O., 2007. Volatile organic compounds in indoor environment and photocatalytic oxidation: state of the art. *Environ. Int.* 33 (5), 694–705.
- Weschler, C.J., 2009. Changes in indoor pollutants since the 1950s. *Atmos. Environ.* 43 (1), 153–169.
- Xiang, Q.J., Lv, K.L., Yu, J.G., 2010. Pivotal role of fluorine in enhanced photocatalytic activity of anatase TiO₂ nanosheets with dominant (001) facets for the photocatalytic degradation of acetone in air. *Appl. Catal. B Environ.* 96 (3–4), 557–564.
- Yin, W.J., Chen, S.Y., Yang, J.H., Gong, X.G., Yan, Y.F., Wei, S.H., 2010. Effective band gap narrowing of anatase TiO₂ by strain along a soft crystal direction. *Appl. Phys. Lett.* 96 (22), 221901.
- Yu, J., Yu, J., Leung, M.K.P., Ho, W.K., Cheng, B., Zhao, X., et al., 2003. Effects of acidic and basic hydrolysis catalysts on the photocatalytic activity and microstructures of bimodal mesoporous titania. *J. Catal.* 217 (1), 69–78.
- Yu, J.G., Yu, H.G., Cheng, B., Zhao, X.J., Zhang, Q.J., 2006. Preparation and photocatalytic activity of mesoporous anatase TiO₂ nanofibers by a hydrothermal method. *J. Photochem. Photobiol. A Chem.* 182 (2), 121–127.
- Yu, J.G., Wang, W.G., Cheng, B., Su, B.L., 2009. Enhancement of photocatalytic activity of mesoporous TiO₂ powders by hydrothermal surface fluorination treatment. *J. Phys. Chem. C* 113 (16), 6743–6750.
- Yuan, S., Sheng, Q., Zhang, J., Chen, F., Anpo, M., 2004. The roles of acid in the synthesis of mesoporous titania with bicrystalline structure. *Mater. Lett.* 58 (22–23), 2757–2760.
- Zhang, H., Banfield, J.F., 2000. Understanding polymorphic phase transformation behavior during growth of nanocrystalline aggregates: insights from TiO₂. *J. Phys. Chem. B* 104 (15), 3481–3487.



Editorial Board of Journal of Environmental Sciences

Editor-in-Chief

X. Chris Le University of Alberta, Canada

Associate Editors-in-Chief

Jiuhui Qu Research Center for Eco-Environmental Sciences, Chinese Academy of Sciences, China
Shu Tao Peking University, China
Nigel Bell Imperial College London, UK
Po-Keung Wong The Chinese University of Hong Kong, Hong Kong, China

Editorial Board

Aquatic environment

Baoyu Gao Shandong University, China
Maohong Fan University of Wyoming, USA
Chihpin Huang National Chiao Tung University, Taiwan, China
Ng Wun Jern Nanyang Environment & Water Research Institute, Singapore
Clark C. K. Liu University of Hawaii at Manoa, USA
Hokyong Shon University of Technology, Sydney, Australia
Zijian Wang Research Center for Eco-Environmental Sciences, Chinese Academy of Sciences, China
Zhiwu Wang The Ohio State University, USA
Yuxiang Wang Queen's University, Canada
Min Yang Research Center for Eco-Environmental Sciences, Chinese Academy of Sciences, China
Zhifeng Yang Beijing Normal University, China
Han-Qing Yu University of Science & Technology of China, China

Terrestrial environment

Christopher Anderson Massey University, New Zealand
Zucong Cai Nanjing Normal University, China
Xinbin Feng Institute of Geochemistry, Chinese Academy of Sciences, China
Hongqing Hu Huazhong Agricultural University, China
Kin-Che Lam The Chinese University of Hong Kong, Hong Kong, China
Erwin Klumpp Research Centre Juelich, Agrosphere Institute, Germany

Peijun Li

Institute of Applied Ecology, Chinese Academy of Sciences, China
Michael Schlöter German Research Center for Environmental Health, Germany
Xuejun Wang Peking University, China
Lizhong Zhu Zhejiang University, China

Atmospheric environment

Jianmin Chen Fudan University, China
Abdelwahid Mellouki Centre National de la Recherche Scientifique, France
Yujing Mu Research Center for Eco-Environmental Sciences, Chinese Academy of Sciences, China
Min Shao Peking University, China
James Jay Schauer University of Wisconsin-Madison, USA
Yuesi Wang Institute of Atmospheric Physics, Chinese Academy of Sciences, China
Xin Yang University of Cambridge, UK

Environmental biology

Yong Cai Florida International University, USA
Henner Hollert RWTH Aachen University, Germany
Jae-Seong Lee Sungkyunkwan University, South Korea
Christopher Rensing University of Copenhagen, Denmark
Bojan Sedmak National Institute of Biology, Slovenia
Lirong Song Institute of Hydrobiology, Chinese Academy of Sciences, China
Chunxia Wang National Natural Science Foundation of China
Gehong Wei Northwest A & F University, China

Daqiang Yin

Tongji University, China
Zhongtang Yu The Ohio State University, USA

Environmental toxicology and health

Jingwen Chen Dalian University of Technology, China
Jianying Hu Peking University, China
Guibin Jiang Research Center for Eco-Environmental Sciences, Chinese Academy of Sciences, China
Sijin Liu Research Center for Eco-Environmental Sciences, Chinese Academy of Sciences, China
Tsuyoshi Nakanishi Gifu Pharmaceutical University, Japan

Willie Peijnenburg University of Leiden, The Netherlands
Bingsheng Zhou Institute of Hydrobiology, Chinese Academy of Sciences, China

Environmental catalysis and materials

Hong He Research Center for Eco-Environmental Sciences, Chinese Academy of Sciences, China
Junhua Li Tsinghua University, China
Wenfeng Shangguan Shanghai Jiao Tong University, China
Ralph T. Yang University of Michigan, USA

Environmental analysis and method

Zongwei Cai Hong Kong Baptist University, Hong Kong, China
Jiping Chen Dalian Institute of Chemical Physics, Chinese Academy of Sciences, China
Minghui Zheng Research Center for Eco-Environmental Sciences, Chinese Academy of Sciences, China
Municipal solid waste and green chemistry
Pinjing He Tongji University, China

Editorial office staff

Managing editor Qingcai Feng
Editors Zixuan Wang Suqin Liu Kuo Liu Zhengang Mao
English editor Catherine Rice (USA)

JOURNAL OF ENVIRONMENTAL SCIENCES

环境科学学报(英文版)

www.jesc.ac.cn

Aims and scope

Journal of Environmental Sciences is an international academic journal supervised by Research Center for Eco-Environmental Sciences, Chinese Academy of Sciences. The journal publishes original, peer-reviewed innovative research and valuable findings in environmental sciences. The types of articles published are research article, critical review, rapid communications, and special issues.

The scope of the journal embraces the treatment processes for natural groundwater, municipal, agricultural and industrial water and wastewaters; physical and chemical methods for limitation of pollutants emission into the atmospheric environment; chemical and biological and phytoremediation of contaminated soil; fate and transport of pollutants in environments; toxicological effects of terrorist chemical release on the natural environment and human health; development of environmental catalysts and materials.

For subscription to electronic edition

Elsevier is responsible for subscription of the journal. Please subscribe to the journal via <http://www.elsevier.com/locate/jes>.

For subscription to print edition

China: Please contact the customer service, Science Press, 16 Donghuangchenggen North Street, Beijing 100717, China. Tel: +86-10-64017032; E-mail: journal@mail.sciencep.com, or the local post office throughout China (domestic postcode: 2-580).

Outside China: Please order the journal from the Elsevier Customer Service Department at the Regional Sales Office nearest you.

Submission declaration

Submission of the work described has not been published previously (except in the form of an abstract or as part of a published lecture or academic thesis), that it is not under consideration for publication elsewhere. The publication should be approved by all authors and tacitly or explicitly by the responsible authorities where the work was carried out. If the manuscript accepted, it will not be published elsewhere in the same form, in English or in any other language, including electronically without the written consent of the copyright-holder.

Editorial

Authors should submit manuscript online at <http://www.jesc.ac.cn>. In case of queries, please contact editorial office, Tel: +86-10-62920553, E-mail: jesc@rcees.ac.cn. Instruction to authors is available at <http://www.jesc.ac.cn>.

Journal of Environmental Sciences (Established in 1989) Volume 32 2015

Supervised by	Chinese Academy of Sciences	Published by	Science Press, Beijing, China
Sponsored by	Research Center for Eco-Environmental Sciences, Chinese Academy of Sciences		Elsevier Limited, The Netherlands
Edited by	Editorial Office of Journal of Environmental Sciences P. O. Box 2871, Beijing 100085, China Tel: 86-10-62920553; http://www.jesc.ac.cn E-mail: jesc@rcees.ac.cn	Distributed by	
		Domestic	Science Press, 16 Donghuangchenggen North Street, Beijing 100717, China Local Post Offices through China
		Foreign	Elsevier Limited http://www.elsevier.com/locate/jes
Editor-in-chief	X. Chris Le	Printed by	Beijing Beilin Printing House, 100083, China

CN 11-2629/X

Domestic postcode: 2-580

Domestic price per issue RMB ¥ 110.00

ISSN 1001-0742

